Available online at www.sciencedirect.com
SCIENCE DIRECT®
Journal of Catalysis 225 (2004) 523–530
JOURNAL OF CATALYSIS
www.elsevier.com/locate/jcat

Alkylation of benzene with ethylene over faujasite zeolite investigated by the ONIOM method

Supawadee Namuangruk, Piboon Pantu, and Jumras Limtrakul *

Laboratory for Computational and Applied Chemistry, Physical Chemistry Division, Kasetsart University, Bangkok 10900, Thailand

Received 30 March 2004; accepted 15 April 2004

Available online 2 June 2004

Abstract

The alkylation of benzene with ethylene over faujasite zeolite has been investigated using an 84T cluster of faujasite zeolite serving as a nanometer-sized chemical reactor modeled by the ONIOM3 (MP2/6-311++G(d,p):HF/6-31G(d):UFF) method, which gives accurate adsorption energies for the reactants and the product, indicating the accuracy of the model in representing interactions between the adsorbates and the zeolite. The computed adsorption energies are −8.73, −13.91, and −20.11 kcal/mol, which compared well with experimentally reported values of −9.0, −14.0, and −20.4 kcal/mol for ethylene, benzene, and ethylbenzene, respectively. Stepwise and concerted mechanisms of the alkylation reaction are considered. For the stepwise mechanism, the alkylation starts with the protonation of the adsorbed ethylene by an acidic zeolite proton leading to the formation of the ethoxide intermediate and, subsequently, the ethoxide reacts with a benzene molecule forming an ethylbenzene product. The computed activation energies are 30.06 and 38.18 kcal/mol for the first and second step, respectively. For the concerted mechanism, the alkylation of benzene takes place in a single reaction step without prior ethoxide formation. The concerted mechanism has an activation energy of 33.41 kcal/mol which is in between the two energy barriers of the stepwise mechanism.

Keywords: Benzene alkylation; Density functional calculations; ONIOM; QM/MM; Zeolite; Reaction mechanism

1. Introduction

Ethylbenzene is an important raw material in the petrochemical industry for the manufacture of styrene, which is one of the most important industrial monomers. Worldwide capacity of ethylbenzene production is about 23 million metric tons per year [1]. Conventionally, ethylbenzene is produced by benzene alkylation with ethylene using mineral acids such as aluminum chloride or phosphoric acid as catalysts. However, these corrosive catalysts cause a number of problems concerning handling, safety, corrosion, and waste disposal. An immense endeavor has been put into developing alternative catalytic systems that are more environmentally friendly. As a result, the ethylbenzene production technology has been progressively moved toward zeolite-based processes. In the past couple of decades, zeolite-based processes have been introduced and licensed by several manufactures, Mobil–Badger, Lummus–UOP, CDTech, and Dow Chemical [1].

Zeolite catalysts also offer an advantage of high selectivity toward the desired product due to the shape-selective properties of their microcrystalline pore structures. Several types of zeolites have been reported to have high activity for benzene alkylation, for example, faujasite, beta, H-ZSM-5, and MCM-22 [1–11]. Elucidation of the reaction mechanism of benzene alkylation on zeolite catalysts is of great interest. From an industry point of view, understanding the alkylation mechanism could help in optimizing the reaction conditions and designing a new catalyst for a more efficient process. However, the reaction mechanism of alkylation of aromatics with short-chain olefins on zeolites is not yet clearly understood. Venuto et al. [2] and Weitkamp [3] suggested that alkylation of benzene with ethylene over acidic faujasite and ZSM-5 zeolites followed the Eley–Rideal mechanism. Corma et al. [4] reported the Eley–Rideal mechanism for alkylation of benzene with propylene over MCM-22. While the Langmuir–Hinshelwood mecha-

* Corresponding author.
E-mail address: fscijrl@ku.ac.th (J. Limtrakul).

0021-9517/$ – see front matter
doi:10.1016/j.jcat.2004.04.016

nism of alkylation of benzene with short-chain olefins has also been reported [5,6]. Recently, Smirniotis and Ruckenstein [7] suggested that the size of the pores of the zeolites in combination with the size of the aromatics and the alkylating agents could regulate the alkylation mechanism. In the case where the size of the aromatic molecule is comparable to the pores of the zeolite, the alkylation proceeds via the Langmuir–Hinshelwood mechanism. For large-pore zeolites such as faujasite and beta zeolites, the alkylation occurs via the Eley–Rideal mechanism.

To clearly envision the reaction mechanism, theoretical study can offer a practical tool that provides insight to the reaction mechanism complementing experimental investigations or, in certain cases, offer an understanding that is not possible by experimental investigations. Numerous theoretical models, including the periodic calculations, have been proposed to study the crystalline zeolite [12–20]. Nevertheless, zeolites that have high impacts in industrial processes usually possess hundreds of atoms per unit cell. This makes the use of sophisticated methods, such as periodic ab initio calculations, that are computationally too expensive and even impractical when very large zeolites are concerned. Therefore, the electronic properties of zeolites are usually modeled with quantum chemical methods for relatively small clusters where only the most important part of zeolites is focused [17–20]. With such limited models, the effect of the framework which can significantly change the structure and energetics of the system is not taken into account. Neglecting the extended framework effect has been shown to lead to discrepancies between the cluster results and the actual zeolite behaviors [21,22]. The recent development of hybrid methods, such as embedded cluster or combined quantum mechanics/molecular mechanics (QM/MM) [14,15,21–25] methods, as well as the more general ONIOM (Our-own-N-layer Integrated molecular Orbital + molecular Mechanics) method [26,27] has brought a larger system within reach of obtaining accurate results.

In our recent studies, the ONIOM model has been successfully employed to study the adsorption of ethylene, benzene, and ethylbenzene over acidic and alkali faujasite and ZSM-5 zeolites [28–31]. The model consisted of an inner layer of active region modeled by a small cluster using the density-functional theory to account for the interactions of the adsorbates with the acid site of zeolite, and a large outer layer of the zeolite framework represented by a molecular mechanics force field to account for the Van der Waals interactions due to confinement of the microporous structure [30–37]. This efficient scheme yielded adsorption energies close to the experimental estimates, suggesting that the ONIOM approach is a sufficiently accurate and practical model in studying adsorption of unsaturated hydrocarbons on zeolites.

In this paper, we have employed the ONIOM method to theoretically study the reaction mechanism of alkylation of benzene with ethylene on an acidic faujasite zeolite. To accurately account for the electron delocalization in the benzene molecule and bond breaking forming during the reaction course, we utilize the second-order Møller–Plesset perturbation theory (MP2) method for the model of the 3T cluster of the zeolite Brønsted acid site and the reactive species. In the intermediate layer, the Hartree–Fock (HF) method is used to complete the remainder of the 12T ring structure of the faujasite pore opening. The outermost layer includes the extended framework properties covering the nanometer-size chemical reactor of 297 atoms of the 84T zeolite structure using the universal force field (UFF).

2. Method

The structure of the 84T cluster, including two supercages, as a nanometer-size chemical reactor where the adsorbates can be trapped inside, is taken from the lattice structure of faujasite zeolite [38]. The ONIOM3 scheme in which the whole model is subdivided into three layers is adapted for computational efficiency. The active region consisting of the 3T cluster, $H_3SiOAl(OH)_2O(H)SiH_3$ (Fig. 1),

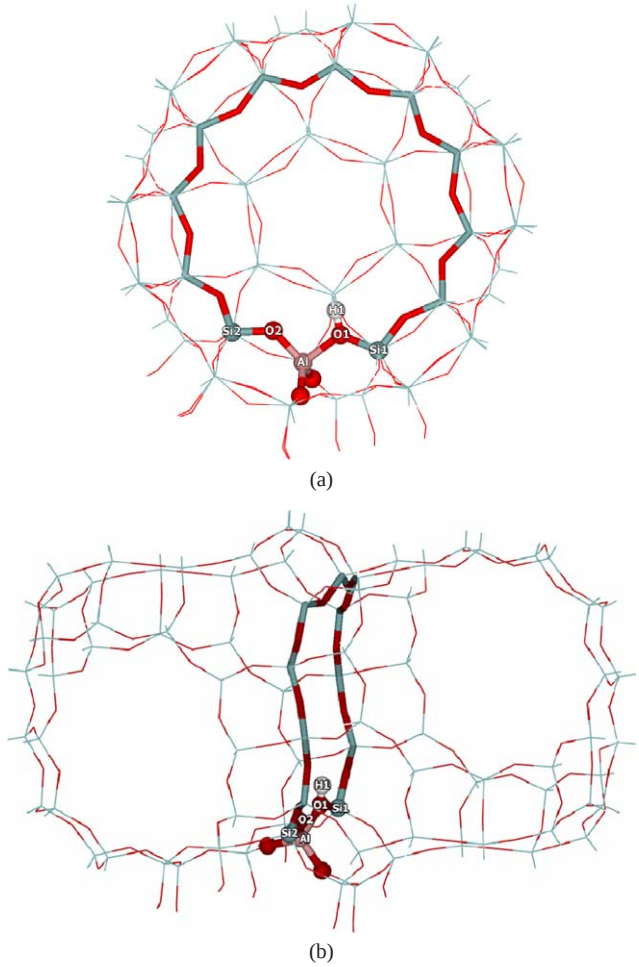

Fig. 1. ONIOM3 layer of 84T cluster models of faujasite. Atoms belongings to the 12T quantum cluster are drawn as bonds and sticks. (a) Front view, (b) side view.

Table 1
The optimized geometric parameters of isolated zeolite clusters (20T and ONIOM model), ethylene adsorption complex, transition state (TS1), and alkoxide intermediate of steps (1) and (2) on FAU using ONIOM3 (distances are in angstroms and angles are in degrees)

Parameters	20T full DFT[a]	Isolated cluster	Ethylene adsorption	TS1	Alkoxide intermediate
Distances					
Al–H1	2.508	2.462	2.471	2.655	–
C1–C2	–	1.335	1.344	1.397	1.502
C1–H1	–	–	2.048	1.204	1.084
C2–H1	–	–	2.119	–	–
O1–H1	0.969	0.970	0.996	1.462	–
C2–O2	–	–	–	2.223	1.521
Al–O1	1.914	1.876	1.856	1.755	1.698
Al–O2	1.700	1.694	1.699	1.773	1.878
Si1–O1	1.704	1.669	1.658	1.614	1.595
Si2–O2	1.608	1.606	1.601	1.625	1.681
Angles					
∠Si1O1Al	123.4	123.7	123.5	122.0	118.1
∠Si2O2Al	129.9	130.4	131.8	132.9	132.8

[a] From Ref. [30].

which is considered the smallest unit required to represent the acid site of zeolite and the reactive molecules, is treated with the MP2/6-31G(d,p) method. In the 3T cluster, one of the silicon atoms in the faujasite zeolite is substituted by an aluminum atom, and a proton is added to one of the bridging oxygen atoms bonded directly to the aluminum atom, conventionally called the O1 position [39]. The extended framework environment is included using less expensive levels of theories, the Hartree–Fock, and molecular mechanics force field (UFF) methods [40]. The HF/3-21G method is used for the 9T ring fragment connecting the 3T acidic site to complete the 12T pore opening of the faujasite zeolite. The rest of the extended framework is treated with the UFF force field to reduce the required computational time and to practically represent the confinement effect of the zeolite pore structure.

All calculations have been performed by using the Gaussian98 code [41]. The basis set for the Hartree–Fock calculations is 3-21G, while the 6-31G(d,p) basis set is used for the MP2 calculations. During the structure optimization, only the active site region [≡SiO(H)Al(O)$_2$OSi≡] and the adsorbates are allowed to relax.

In order to obtain more reliable interaction energies, the single-point energy calculations at the ONIOM(MP2/6-311++G(d,p):HF/6-31G(d):UFF)//ONIOM(MP2/6-31G(d,p):HF/3-21G:UFF) level are carried out and basis set superposition error (BSSE) corrections are also taken into account.

3. Results and discussion

Recent studies [28–37] have shown that the Van der Waals interactions between hydrocarbon and aromatic adsorbates and the zeolite wall contribute significantly to the energetic of the adsorption–desorption process in zeolites. Consequently, typical small quantum cluster calculations which basically neglect these interactions result in erroneous adsorption energies. On the other hand, the hybrid methods such as QM/MM and ONIOM can reasonably describe the interactions with the zeolite framework and have been reported to give adsorption energies close to experimental values [28–31]. Therefore, in this work we use the ONIOM method to investigate the alkylation of benzene with ethylene over faujasite zeolite.

3.1. Model of faujasite catalyst

In this work, we employ the 3-layered ONIOM method for investigating the reaction mechanism of alkylation of benzene with ethylene. To accurately account for the electron delocalization in the benzene molecule and bond breaking forming during the reaction course, the MP2 method is used for the model of the 3T cluster of zeolite Brønsted acid sites and the reactive species. The HF method is used to complete the 12T ring structure of the faujasite pore opening and the UFF force field is used to model the extended framework effect covering the 84T extended zeolite structure. The structure of the zeolite model is presented in Fig. 1 and selected structural parameters are tabulated in Table 1. The structure of the active site obtained from the 3-layered ONIOM model is in reasonable agreement with the structure obtained from our previous study [30] of the 20T full quantum cluster optimized at B3LYP/6-31G(d,p) level theory (see Table 1). The Brønsted O1–H1 and Al–O1 and Si1–O1 bond distances are very close to the values reported in our previous calculations [30]. Further support for the reliability of the active site subunit, ≡SiO(H)Al(O)$_2$OSi≡, is given from the NMR measurements that the internuclear distance between the aluminum and proton nuclei in a Brønsted acid site, r(Al···H), of faujasite which is reported to be 2.38 ± 0.04 Å [42] and, more recently, 2.48 ± 0.04 Å [39] and our computed r(Al···H)

is 2.462 Å, which is reasonably close to the experimentally measured value.

3.2. Adsorption of the reactant and product molecules on the Brønsted acid site

Ethylene weakly adsorbs onto the zeolite acid site via π-interaction. The weak interaction does not significantly perturb the structure of ethylene and the zeolite. Upon the adsorption of ethylene, only minor changes of the zeolite structure were detected (less than 0.03 Å and 2° for changes in bond distances and bond angles, respectively). Nevertheless, the C–C double bond distance of the ethylene molecule is increased slightly from 1.335 to 1.344 Å and the acidic O1–H1 bond distance is increased from 0.970 to 0.996 Å, indicating that the adsorption slightly weakens the C–C double bond and the acidic O1–H1 bond, which may lead to the protonation of ethylene and the formation of the alkoxide intermediate. The adsorption energy is computed to be −8.73 kcal/mol, which compared well with the experimental observation of −9.0 kcal/mol [43].

Benzene and ethylbenzene also weakly interact with the zeolite acid site via π-interaction. The C–C double bond in the benzene ring that forms the π-interaction with the zeolite is slightly increased and the acidic O1–H1 bond distance is slightly increased from 0.970 to 0.985 Å for both benzene and ethylbenzene adsorption complexes, respectively. Similar to the adsorption of ethylene, the zeolite structural parameters are slightly changed by the weak interactions (changes in bond distances and bond angles are less than 0.02 Å, and 2°, respectively). Obviously, the Van der Waals interaction for the case of benzene is weaker than for the ethylbenzene adsorption and, hence, the corresponding adsorption energies are −13.91 and −20.11 kcal/mol for benzene and ethylbenzene, respectively. These values are very close to the experimental values of −14.0 [44] and −20.4 kcal/mol [45] for adsorption of benzene and ethylbenzene in H–Y zeolites, respectively.

The accurately predicted adsorption energies clearly demonstrate that the ONIOM3 model used in this work can represent interactions between the adsorbates and zeolite very well. The combination of the MP2 method at the active region embedded in the extended structure modeled by the HF and UFF methods apparently works well in representing electron correlation, electrostatic, and Van der Waals interactions in the zeolite system.

3.3. Reaction mechanism for benzene alkylation with ethylene

Recently, several reports have supported that benzene alkylation with light olefins in medium and large-pore zeolite catalysts occurs via the Eley–Rideal-type mechanism. The reaction can be considered to occur either by a concerted mechanism or by a stepwise mechanism through the formation of an alkoxide intermediate before the alkylation of benzene.

3.3.1. Stepwise mechanism for benzene alkylation with ethylene

The alkylation of benzene with ethylene in faujasite zeolite can be viewed to proceed according to following steps:

$$C_2H_4 + H\text{–}FAU \rightleftharpoons C_2H_4\text{–}H\text{–}FAU, \quad (1)$$

$$C_2H_4\text{–}H\text{–}FAU \rightleftharpoons CH_3CH_2\text{–}FAU, \quad (2)$$

$$CH_3CH_2\text{–}FAU + C_6H_6 \rightleftharpoons (CH_3CH_2)C_6H_5\text{–}H\text{–}FAU, \quad (3)$$

$$(CH_3CH_2)C_6H_5\text{–}H\text{–}FAU \rightleftharpoons (CH_3CH_2)C_6H_5 + H\text{–}FAU. \quad (4)$$

Step (1) is the adsorption of ethylene on the acid site of the zeolite. Then, in step (2), protonation of the adsorbed ethylene occurs, leading to the formation of an ethoxide intermediate. Step (3) involves the interaction of the alkoxide intermediate with benzene, resulting in adsorbed ethylbenzene which is desorbed in the final step. Under typical reaction temperatures, ethylene readily adsorbs on the zeolite acid site and interacts strongly to the Brønsted acid site. On the other hand, the adsorbed benzene weakly interacts with the acid site (although the benzene adsorption energy is high, most of it derives from Van der Waals interactions with the zeolite pore walls) [46,47]. In addition, with the adsorption experiments reported in the literature [48,49] it can be concluded that the adsorption constant for benzene is small; therefore, it is possible to assume, for simplicity, that the competitive adsorption of benzene can be considered unimportant.

Fig. 2a shows the calculated energy profile for the reactions in steps (1) and (2) and Table 1 shows selected geometric parameters of the intermediates and transition state. Ethylene weakly adsorbs on the acid site via π-interaction with the adsorption energy of −8.73 kcal/mol. The weakly adsorbed ethylene can be protonated by the acidic proton. The protonated ethylene is, however, not stable in a form of carbenium ion and, hence, it is quickly transformed to a stabilized alkoxide intermediate by forming a covalent bond to one of the bridging oxygen atoms. At the transition state (Fig. 2b) there is one imaginary frequency at 619 cm^{-1} corresponding to the following movements: the zeolite proton is moving toward a carbon atom of the ethylene while the C–C double bond of the ethylene is elongated from 1.344 to 1.397 Å and the other carbon atom is moving toward the adjacent oxygen atom of the zeolite framework to form a covalent bond. The energy barrier for the protonation is calculated to be 30.06 kcal/mol and the apparent activation energy for this step is 21.33 kcal/mol. The computed apparent activation energy is in reasonable agreement with the estimated range of apparent activation energy for the isotope exchange of ethylene in zeolites of 15–20 kcal/mol reported in the literature [43,50]. The formation of the covalent bonded ethoxide species is accompanied by significant structural changes of the zeolite. The Al–O1 and Si1–O1

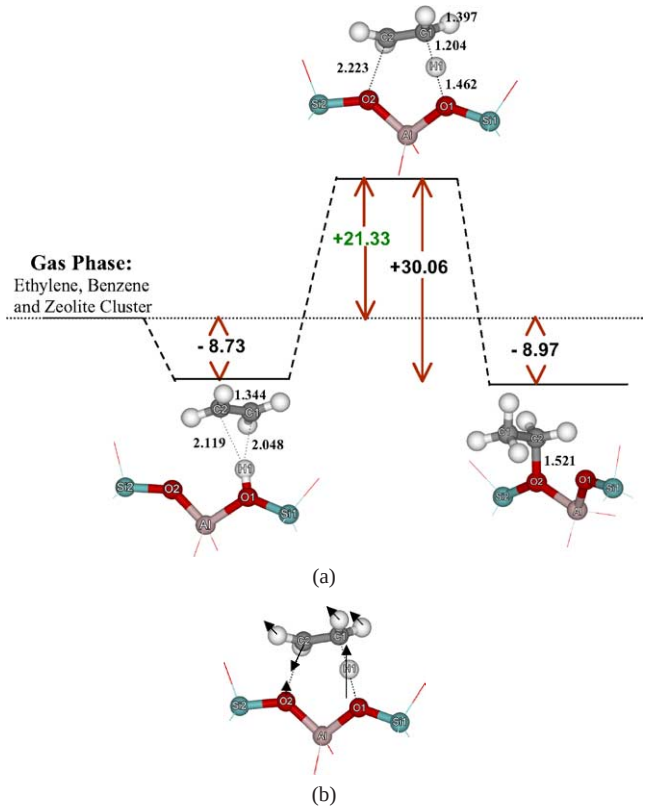

Fig. 2. (a) Calculated energy profile for the stepwise reactions in steps (1) and (2). (b) Vibrational movement corresponding to the imaginary frequency at the transition structure of step (2).

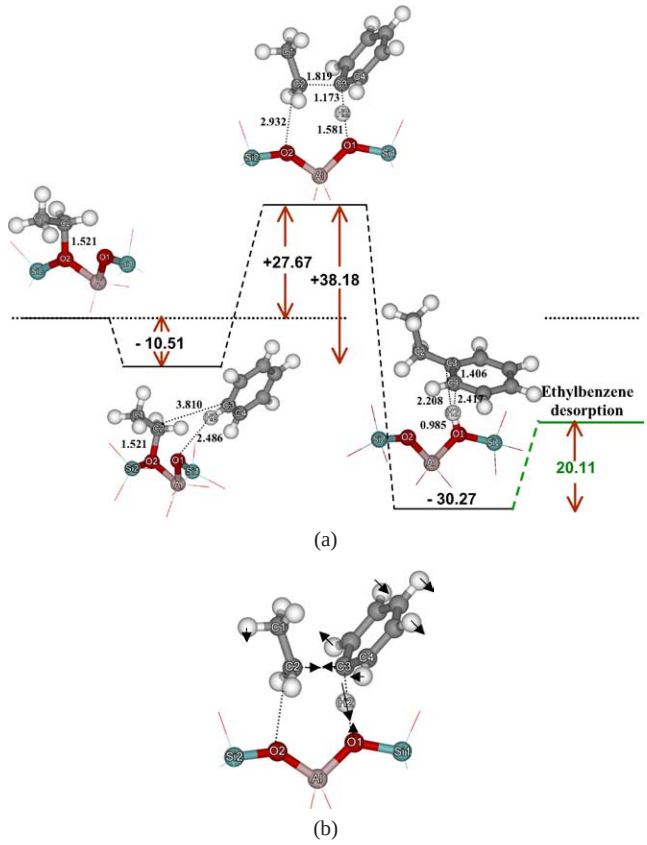

Fig. 3. (a) Calculated energy profile for the stepwise reactions in steps (3) and (4). (b) Vibrational movement corresponding to the imaginary frequency at the transition structure of step (3).

bond distances are decreased by 0.178 and 0.074 Å, respectively, as the Si1–O1–Al bond angle is decreased by 5.6°. While, the Al–O2 and Si2–O2 bond distances are increased by 0.184 and 0.075 Å, respectively, as the Si1–O2–Al bond angle is increased by 2.4° (Table 1). Rozanska et al. [51] have shown that when the zeolite framework is modeled by an unrealistic constraint model, erroneous results can be obtained. In the ONIOM model, the small cluster of the active region is generally connected to the outer layer of the system via fixed anchoring atoms. Therefore, only a number of atoms at the active site region can be relaxed. In our model, although only atoms belonging to the active site region [≡SiO(H)Al(O)$_2$OSi≡] are allowed to relax, the energetic properties of the system, e.g., adsorption energies, and activation energy for ethylene protonation, are reasonable and compared well with previously reported values by experimental measurements and theoretical calculations [43–45], indicating the validity of the model. It has been shown that the stability of alkoxide intermediates formed in the zeolite structure is very sensitive to the local geometry of the active site [52]. When the geometry of the system is modeled to represent a particular zeolite structure, the covalent bond between the alkoxide species and the zeolite is weakened and the alkoxide is greatly destabilized due to the steric constraints of the zeolite pore walls [51,52]. In this model, the 3T cluster of the active site is embedded into the 84T crystal lattice of faujasite zeolite and, hence, it inherits the steric constraints of the nanostructured zeolite pores. As a result, the alkoxide intermediate in this model appears to be an active species that can readily become involved in the benzene alkylation.

Table 2
The optimized geometric parameters of benzene–alkoxide adsorption complex, transition state (TS2), and product ethylbenzene adsorption of step (3) on FAU using ONIOM3 (distances are in angstroms and angles are in degrees)

Parameters	Benzene–alkoxide	TS2	Product
Distances			
C1–C2	1.501	1.505	1.531
C2–C3	3.810	1.819	1.509
C3–C4	1.395		1.406
C3–H2	1.082	1.173	2.208
C4–H2	1.079		2.417
O1–H2	2.486	1.581	0.985
C2–O2	1.521	2.932	3.693
Al–O1	1.701	1.730	1.858
Al–O2	1.881	1.775	1.698
Si1–O1	1.598	1.591	1.665
Si2–O2	1.682	1.608	1.599
Angles			
∠Si1O1Al	118.4	121.2	122.9
∠Si2O2Al	133.1	136.7	132.1

The reaction profile involving the reaction between the alkoxide intermediate with benzene to produce ethylbenzene is shown in Fig. 3a and selected structural parameters are tabulated in Table 2. A benzene molecule diffuses into the vicinity to react with the alkoxide. The alkylation of benzene involves concerted bond forming between the carbon atoms of ethylene and benzene and the breaking of a benzene proton giving the proton back to the zeolite-bridging oxygen. The vibrational motion corresponding to the imaginary frequency at the transition is explicitly shown in Fig. 3b, which clearly demonstrates that the C–C bond forming between the ethyl and benzene occurs via interactions of surface ethoxide and benzene. During the transformation, the C–O covalent bond of the surface ethoxide is breaking while the bond between the ethyl and benzene begins to form and a benzene proton is leaving toward the zeolite framework. The activation energy is evaluated to be 38.18 kcal/mol. The adsorbed ethylbenzene product is subsequently desorbed endothermically, requiring energy of 20.11 kcal/mol.

3.3.2. *Concerted mechanism for benzene alkylation with ethylene*

Alternatively, benzene alkylation can proceed via concerted interactions in the coadsorbed complex of ethylene and benzene without the formation of an alkoxide intermediate. The reaction steps can be written as follows:

$$C_2H_4 + H\text{–}FAU \rightleftharpoons C_2H_4\text{–}H\text{–}FAU, \quad (5)$$

$$C_6H_6 + C_2H_4\text{–}H\text{–}FAU \rightleftharpoons (CH_3CH_2)C_6H_5\text{–}H\text{–}FAU, \quad (6)$$

$$(CH_3CH_2)C_6H_5\text{–}H\text{–}FAU \rightleftharpoons (CH_3CH_2)C_6H_5 + H\text{–}FAU. \quad (7)$$

Very recently, DFT cluster calculations of ethylbenzene formation via the concerted reaction of the coadsorbed complex have been reported using DFT quantum cluster calculations by Vos et al. [53] and Arstad et al. [54]. Therefore, a comparison will be made and the effect of inclusion of the extended framework of the zeolite by the ONIOM method will be discussed.

The reaction energy profile is presented in Fig. 4a and the selected geometrical parameters of intermediates and transition state are tabulated in Table 3. The reaction is initiated by coadsorption of benzene on the adsorbed ethylene at the acid site of the zeolite. The coadsorption energy is evaluated to be −16.79 kcal/mol, which is significantly higher than the values previously reported by Vos et al. and Arstad et al. (7.3 and 7.8 kcal/mol, respectively). The difference results mainly from Van der Waals interactions between the adsorbed complex and the zeolite walls, which in this study were taken into account by using the UFF force field to model the extended framework of the zeolite [30–37]. At the transition state, there is an imaginary frequency associated with the transition complex (Fig. 4b) which indicates that the zeolitic proton (H1) is moving toward the ethylene carbon (C1) and the other ethylene carbon (C2) starts forming a bond with the benzene carbon (C3) and, simultaneously, the

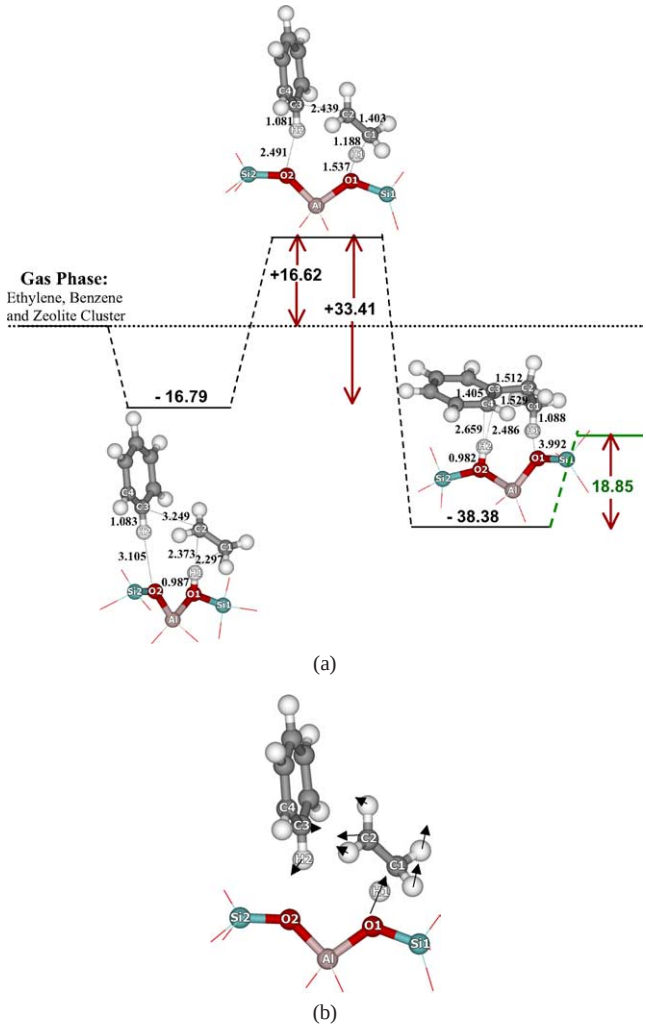

Fig. 4. (a) Calculated energy profile for the concerted reactions. (b) Vibrational movement corresponding to the imaginary frequency at the transition structure.

benzene proton is leaving toward the zeolite-bridging oxygen (O2). The vibrational motion of the transition state complex clearly indicates the concerted mechanism of the alkylation of benzene. The structure of the transition state shows that the Brønsted acid O1–H1 distance is greatly lengthened from 0.987 to 1.537 Å and the distance between the zeolitic proton (H1) and the ethylene carbon (C1) becomes 1.188 Å. The ethylene C–C bond distance is significantly lengthened from 1.342 to 1.403 Å, whereas the structure of the benzene molecule does not significantly differ from that of the coadsorbed structure except that the distance between the benzene proton (H2) and the zeolite-bridging oxygen (O2) is shortened from 3.105 to 2.491 Å. The transition-state structure obtained in this model is similar to that of reported by Arstad et al., but slightly different from that reported by Vos et al. in which the ethylene is completely protonated at the transition state. The activation energy is calculated to be 33.41 kcal/mol, very close to the numbers reported by Vos et al. and Arstad et al. (31.6 and 31.3 kcal/mol, respectively).

Table 3
The optimized geometric parameters of isolated molecule, coadsorption complex, transition state (TS), and product of concerted reaction of benzene alkylation on FAU using ONIOM3 (distances are in angstroms and angles are in degrees)

Parameters	Isolated cluster	Coadsorption complex	Transition state	Product
Distances				
Al–H1	2.462			
C1–C2	1.335	1.342	1.403	1.529
C2–C3	–	3.249	2.439	1.512
C3–C4	–	1.398	1.408	1.405
C3–H2	–	1.083	1.081	2.486
C4–H2	–	2.147	2.159	2.659
O2–H2	–	3.105	2.491	0.982
C1–H1	–	2.297	1.188	1.088
C2–H1		2.373	2.030	2.165
O1–H1	0.970	0.987	1.537	3.992
Al–O1	1.876	1.861	1.773	1.701
Al–O2	1.694	1.699	1.741	1.886
Si1–O1	1.669	1.667	1.612	1.601
Si2–O2	1.606	1.602	1.598	1.683
Angles				
∠Si1O1Al	123.7	122.9	121.7	116.9
∠Si2O2Al	130.4	131.5	134.9	135.1

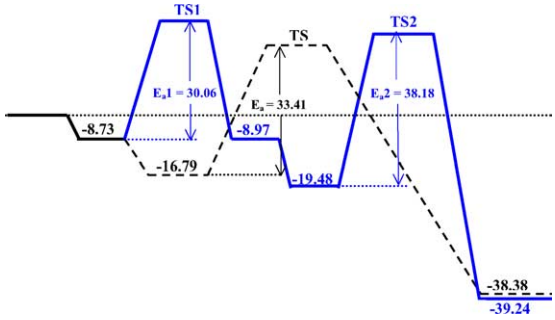

Fig. 5. Calculated energetic profiles for the stepwise (solid line) and concerted (dashed line) reaction mechanisms.

The complete energetic profiles of the two mechanisms are drawn on the same diagram (Fig. 5) for easy comparison. For the stepwise mechanism, the alkoxide formation has a smaller activation energy of 30.06 kcal/mol and the surface reaction step is the rate-determining step with the activation energy of 38.18 kcal/mol. The activation barrier of the concerted mechanism of 33.41 kcal/mol is in between the barriers of the stepwise mechanism. It might appear that the concerted mechanism should dominate the overall alkylation reaction due to the smaller activation energy. However, the stepwise mechanism could also contribute significantly because, from an energetic point of view, the alkoxide formation will occur relatively easily, and after the alkoxide intermediate is formed the stability of the adsorbed benzene–alkoxide adduct makes the reverse reaction more difficult to occur than the forward reaction to the ethylbenzene product. When it is considered that both mechanisms can take place under the reaction conditions, the calculated apparent activation energy for the alkylation of benzene with ethylene would be in a range of 16.62–27.67 kcal/mol. Although, there is no experimental value of the activation energy for alkylation of benzene with ethylene in zeolites to compare with, our computed apparent activation energy range seems reasonable when compared with the apparent activation energies (10–18 kcal/mol) for alkylation of benzene with propylene in zeolites [4,6,46]. Because ethylene is a poorer alkylating agent than propylene, and the rate of benzene alkylation with ethylene is much slower than that with propylene and generally it requires a higher reaction temperature to obtain the same conversion level as that of the alkylation with propylene [1,4,47,53], the activation energy of the alkylation with ethylene is expected to be higher than the activation energy of the alkylation with propylene.

4. Conclusion

The alkylation of benzene with ethylene over faujasite zeolite has been investigated using the ONIOM3 model. The model is shown to be accurate in predicting adsorption energies of the adsorbed reactants and product compared to experimental estimates. Two alkylation mechanisms, stepwise and concerted, are considered. For the stepwise mechanism, the alkylation starts with protonation of the adsorbed ethylene which leads to the formation of the active surface ethoxide intermediate. Benzene alkylation takes place via interactions between the ethoxide species and a benzene molecule. The rate-determining step is found to be the reaction step where concerted bond forming between the carbon of the ethyl fragment and benzene and bond breaking of a benzene proton occur. The activation energy of 38.18 kcal/mol is predicted. For the concerted mechanism, the alkylation of benzene takes place in a single reaction step of the coadsorbed reactants without prior alkoxide formation. The activation energy is calculated to be 33.41 kcal/mol.

The results derived in the present study suggest that the ONIOM approach yields an accurate and practical model

for exploring the structure, adsorption, and reaction mechanisms of zeolites.

Acknowledgments

This work was supported in part by grants from the Thailand Research Fund (TRF Senior Research Scholar to J.L.) and the Kasetsart University Research and Development Institute (KURDI), as well as the Ministry of University Affairs under the Science and Technology Higher Education Development Project (MUA-ADB funds). The support from the Dow Chemical Company (USA) is also acknowledged.

References

[1] T.F. Degnan Jr., C.M. Smith, C.R. Venkat, App. Catal. A 221 (2001) 283.
[2] P.B. Venuto, L.A. Hamilton, P.S. Landis, J. Catal. 5 (1966) 484.
[3] J. Weitkamp, Int. Sympos. in Zeolite Catalysis, Siofok, Hungary, Acta Phys. Chem. 217 (1985).
[4] A. Corma, V. Martinez-Soria, E. Schnoeveld, J. Catal. 192 (2000) 163.
[5] Y. Morita, H. Matsumoto, T. Kimura, F. Kato, M. Takayasu, Bull. Jpn. Pet. Inst. 15 (1) (1973) 37.
[6] K.A. Becker, H.G. Karge, W.-D. Streubel, J. Catal. 28 (1973) 403.
[7] P.G. Smirniotis, E. Ruckenstein, Ind. Eng. Chem. Res. 34 (1995) 1517.
[8] W.W. Kaeling, R.E. Holland, J. Catal. 19 (1988) 212.
[9] N.Y. Chen, W.E. Garwood, Catal. Rev.-Sci. Eng. 28 (1986) 185.
[10] K.S.N. Reddy, B.S. Rao, U.P. Shiralkar, Appl. Catal. A 95 (1993) 53.
[11] A. Corma, Chem. Rev. 95 (1995) 559.
[12] R. Shah, J.D. Gale, M.C. Payne, J. Phys. Chem. B 101 (24) (1997) 4787.
[13] Y. Jeanvoine, J.G. Angyan, G. Kresse, J. Hafner, J. Phys. Chem. B 102 (1998) 5573.
[14] I.H. Hillier, J. Mol. Struct. (Theochem.) 463 (1999) 45.
[15] J. Limtrakul, S. Jungsuttiwong, P. Khongpracha, J. Mol. Struct. 525 (2000) 153.
[16] J. Sauer, M. Sierka, J. Comput. Chem. 21 (2000) 1470.
[17] J. Sauer, P. Ugliengo, E. Garrone, V.R. Saunders, Chem. Rev. 94 (1994) 2095.
[18] J. Sauer, Chem. Rev. 89 (1989) 199.
[19] J. Limtrakul, Chem. Phys. 193 (1995) 79.
[20] J. Limtrakul, P. Treesukol, C. Ebner, M. Probst, Chem. Phys. 215 (1997) 77.
[21] P.E. Sinclair, A.H. de Vries, P. Sherwood, C.R.A. Catlow, R.A. van Santen, J. Chem. Soc., Faraday Trans. 94 (1998) 3401.
[22] M. Brandle, J. Sauer, J. Am. Chem. Soc. 120 (1998) 1556.
[23] S.P. Greatbanks, I.H. Hillier, N.A. Burton, P. Sherwood, J. Chem. Phys. 105 (1996) 3370.
[24] R.Z. Khaliullin, A.T. Bell, V.B. Kazansky, J. Phys. Chem. A 105 (2001) 10,454.
[25] J. Limtrakul, T. Nanok, P. Khongpracha, S. Jungsuttiwong, T.N. Truong, Chem. Phys. Lett. 349 (2001) 161.
[26] A.H. de Vries, P. Sherwood, S.J. Collins, A.M. Rigby, M. Rigutto, G.J. Kramer, J. Phys. Chem. B 103 (1999) 6133.
[27] M. Svensson, S. Humbel, R.D.J. Froese, T. Matsubara, S. Sieber, K. Morokuma, J. Phys. Chem. 100 (1996) 19357.
[28] C. Raksakoon, J. Limtrakul, J. Mol. Struct. (Theochem.) 631 (2003) 147.
[29] W. Panjan, J. Limtrakul, J. Mol. Struct. 654 (2003) 35.
[30] S. Kasuriya, S. Namuangruk, P. Treesukol, M. Tirtowidjojo, J. Limtrakul, J. Catal. 219 (2003) 320.
[31] K. Bobuatong, J. Limtrakul, Appl. Catal. A 253 (2003) 49.
[32] A. Pelmenschikov, J. Leszczynski, J. Phys. Chem. B 103 (1999) 6886.
[33] T.A. Wesolowski, O. Parisel, Y. Ellinger, J. Weber, J. Phys. Chem. A 101 (1997) 7818.
[34] E.G. Derouane, C.D. Chang, Mesopor. Mater. 35–36 (2000) 425.
[35] L.A. Clark, M. Sierka, J. Sauer, J. Am. Chem. Soc. 125 (2003) 2136.
[36] A.M. Vos, X. Rozanska, R.A. Schoonheydt, R.A. van Santen, F. Hutschka, J. Hafner, J. Am. Chem. Soc. 123 (2001) 2799.
[37] X. Rozanska, R. A van Santen, F. Hutschka, J. Hafner, J. Am. Chem. Soc. 123 (2001) 7655.
[38] D.H. Olson, E. Dempsey, J. Catal. 13 (1969) 221.
[39] J.R. Hill, C.M. Freeman, B. Delley, J. Phys. Chem. A 103 (1999) 3772.
[40] A.K. Rappe, C.J. Casewit, K.S. Colwell, W.A. Goddard, W.M. Skiff, J. Am. Chem. Soc. 114 (1992) 10,024.
[41] M.J. Frisch, G.W. Trucks, H.B. Schlegel, G.E. Scuseria, M.A. Robb, J.R. Cheeseman, V.G. Zakrzewski, J.A. Montgomery, R.E. Stratmann Jr., J.C. Burant, S. Dapprich, J.M. Millam, A.D. Daniels, K.N. Kudin, M.C. Strain, O. Farkas, J. Tomasi, V. Barone, M. Cossi, R. Cammi, B. Mennucci, C. Pomelli, C. Adamo, S. Clifford, J. Ochterski, G.A. Petersson, P.Y. Ayala, Q. Cui, K. Morokuma, P. Salvador, J.J. Dannenberg, D.K. Malick, A.D. Rabuck, K. Raghavachari, J.B. Foresman, J. Cioslowski, J.V. Ortiz, A.G. Baboul, B.B. Stefanov, G. Liu, A. Liashenko, P. Piskorz, I. Komaromi, R. Gomperts, R.L. Martin, D.J. Fox, T. Keith, M.A. Al-Laham, C.Y. Peng, A. Nanayakkara, M. Challacombe, P.M.W. Gill, B. Johnson, W. Chen, M.W. Wong, J.L. Andres, C. Gonzalez, M. Head-Gordon, E.S. Replogle, J.A. Pople, Gaussian98, Gaussian, Pittsburgh, PA, 2001.
[42] D. Freude, J. Klinowski, H. Hamdan, Chem. Phys. Lett. 149 (1988) 355.
[43] N.W. Cant, W.K. Hall, J. Catal. 25 (1972) 161.
[44] D. Barthomeuf, B.H. Ha, J. Chem. Soc., Faraday Trans. 112 (1973) 2158.
[45] D.M. Ruthven, M. Goddard, Zeolites 6 (1978) 275.
[46] S. Siffert, L. Gaillard, B.-L. Su, J. Mol. Catal. A 153 (2000) 267.
[47] Y. Du, H. Wang, S. Chen, J. Mol. Catal. A 179 (2002) 253.
[48] P.B. Venuto, P.S. Landis, Adv. Catal. 18 (1968) 259.
[49] C. Flego, I. Kiricsi, C. Perego, G. Bellussi, Stud. Surf. Sci. Catal. 94 (1995) 405.
[50] E.M. Evleth, E. Kassab, H. Jessri, M. Allavena, L. Montero, L.R. Sierra, J. Phys. Chem. 100 (1996) 11,368.
[51] X. Rozanska, Th. Demuth, F. Hutschka, J. Hafner, R.A. van Santen, J. Phys. Chem. B 106 (2002) 3248.
[52] M. Boronat, C.M. Zircovich-Wilson, P. Viruela, A. Corma, J. Phys. Chem. B 105 (2001) 11,169.
[53] A.M. Vos, R.A. Schoonheydt, F.D. Proft, P. Geerlings, J. Phys. Chem. B 107 (2003) 2001.
[54] B. Arstad, S. Kolboe, O. Swang, J. Phys. Chem. B 108 (2004) 2300.